EasyChair Preprint

№ 13168

Low-Cycle Fatigue Performances Including Large Plastic Strain of SUS821L1 Lean Duplex Stainless Steel

Thaileang Touch, Shoichi Kishiki and Satoshi Yamada

May 2, 2024

Low-Cycle Fatigue Performances Including Large Plastic Strain of SUS821L1 Lean Duplex Stainless Steel

Thaileang Touch[1], Shoichi Kishiki[2] and Satoshi Yamada[3]

[1] Fujita Corporation, (Former graduate student at Tokyo Institute of Technology), 4-25-2 Sendagaya, Shibuya-ku, Tokyo 151-8570, Japan
touch.thaileang@fujita.co.jp
[2] Institute of Innovative Research, Tokyo Institute of Technology, J2-21, 4259 Nagatsuta, Midori-ku, Yokohama 226-8503, Japan
[3] Department of architecture, The University of Tokyo, 7-3-1, Hongo, Bunkyo-ku, Tokyo, 113-8656, Japan

Abstract. Owing to the high corrosion resistance and high strength-to-mass ratio, lean duplex stainless steel is expected to contribute to increased strength and reduction of the component thickness, helping to achieve light weight structural design goal. When considering the use of lean duplex stainless steel in the main component, it is necessary to investigate the seismic performance of structures. In such a case, the material level of the main component under strong earthquake is subjected to a larger strain. To date, however, test data on duplex stainless steel is limited to ±5% or less, which is insufficient to analyze the response of stainless-steel structures in large plastic strain during strong earthquakes. This paper investigates the low-cycle fatigue (LCF) performances, including large strains (> ±5%), of SUS821L1 lean duplex stainless steel at the material level. It was tested under constant strain amplitudes from ±2% to ±12%. The obtained results were compared with previous studies considering stainless and carbon steels. The results showed SUS821L1 has significantly higher yield and tensile strengths than other steels. Besides, the LCF performance of SUS821L1 differs from that of other steels. It was confirmed that this difference can be explained using the skeleton and Bauschinger parts decomposed from hysteretic curves.

Keywords: Lean Duplex Stainless Steel, Low-Cycle Fatigue, Large Plastic Strain, Skeleton Curve, Bauschinger Part.

1 Introduction

Stainless steels can be used for structures in severe corrosive environments because of their excellent corrosion resistance. Austenitic stainless steel, which is representative of stainless steels, are widely used in structure. However, compared to austenitic stainless steel, duplex stainless steels have higher corrosion resistance, and its yield strength is about two times higher [1]. Moreover, lean duplex stainless steels, which are oriented toward price stability by reducing the rare elements Ni and Mo, have corrosion

resistance equivalent to or better than austenitic steels. The strength of the lean duplex stainless steel is also comparable to the duplex stainless steel [1]. The lean duplex stainless steel which is more affordable than duplex stainless steel was included in the JIS [2] in 2015.

When considering the use of lean duplex stainless steel in the main component, it is essential to investigate the seismic performance of structures. Furthermore, under large earthquakes, the material level of the main structural member will be subjected to large strains [3,4]. Therefore, it is important to understand the low-cycle fatigue performance of low-alloy duplex stainless steels including large strains. Previously, Udo et al. [5] and Horisawa et al. [6] conducted experimental studies on fatigue strength for various stainless steels and stress ratios, including lean duplex stainless steels. However, their investigations were limited to the high-cycle fatigue regime in the elastic range. In the low-cycle fatigue (LCF) regime, the steel material deforms inelastically, and the experimental studies are conducted with strain-controlled tests. Regarding the studies in low-cycle fatigue regime, Alvarez-Armas et al. [7] performed experiments on three duplex stainless steels with strains ranging from ±0.2% to ±1% and proposed the LCF evaluation equations. Zhang et al. [8] performed cyclic loading tests with higher strains (up to ±2.5%). However, the study [8] mainly focused on the fracture properties of base metal and weld metal of duplex stainless steels. Besides, Chang et al. [9] conducted experiments up to about 12% strain on specimens with circular cross sections to study hysteretic model and predictive model for fracture of the duplex stainless steels. Nevertheless, the compressive strain was set to zero since buckling is of concern. This means that ±6% can be considered for a fully reversed amplitude. To further investigate the LCF performance, Chen et al [10] used a rectangular section specimen made of duplex stainless steel and subjected it to cyclic loading with strains from ±0.5% to ±5%. In the experiments, the specimens were stiffened with buckling restraint plates to reduce the buckling susceptibility of the rectangular cross sections.

For the reasons mentioned above, it is evident that there has been a lot of interest in the study on the LCF performance, including large strain, of lean duplex stainless steels and duplex stainless steels for structural applications. However, at present, there are few studies on the LCF performance of lean duplex stainless steels. Even in studies of duplex stainless steels, experimental data were conducted up to ±6% strain, which is inadequate to comprehend the seismic performance of stainless steel building structures in the large strain region that the member's material level experiences during a major earthquake.

The purpose of this study is to clarify the low-cycle fatigue performance of SUS821L1 lean duplex stainless steel, including large strains at the material level. First, to obtain experimental data of LCF, cyclic loading tests with constant strain amplitudes from ±2% to ±12% for fully reversed amplitude and from 4% to 24% for zero offset amplitude are conducted on a circular cross-section specimen. Based on the obtained results, LCF performance evaluation equations are proposed and compared with the LCF performance of various steels used in [11]. The differences in LCF performance of different steels are also discussed in terms of the skeleton curve and Bauschinger part, which are decomposed from the hysteretic curve.

2 Testing method

The target steel for this study is the SUS821L1 lean duplex stainless steel. Tables 1 and 2 show the chemical composition and mechanical properties of various strain steels. Test data for SS400, SM490A, and SA440C carbon steels from previous study [11] using the same specimen geometry are also used for comparison. The nominal stress-nominal strain relationship obtained from the monotonic tensile tests of these steels is shown in Fig. 1. 0.2% offset was used as the yield point for SUS821L1 and SA440C, since no distinct yield plateau appeared.

The specimen geometry and test setup are shown in Fig. 2. The determination of the specimen shape can be referred in previous studies [11,12]. Two loading histories (Fig. 3) were performed under axial strain control: offset amplitude (strain ratio = 0) and fully reversed amplitude (strain ratio = -1) to investigate the effect of strain ratio (compressive strain/tensile strain) on the LCF performance.

A universal testing machine (load capacity of 500 kN) was used to apply axial deformation. Extensometers were installed at the effective length section, and strain gauges were attached to the front and back of the specimens as shown in Fig. 2. Loading test was controlled by the true strain calculated from the extensometer readings under the assumption of constant volume. The range of loading strain amplitude was ±2% to ±12% for fully reversed amplitude ($\Delta\varepsilon/2$) and 4% to 24% for the zero offset amplitude ($\Delta\varepsilon$).

Table 1 Chemical compositions of stainless steel

Steel materials (JIS standard [2])	C	Si	Mn	P	S	Ni	Cr	Mo	Cu	N	Co
SUS304	0.08	1	2	0.045	0.03	8-10.5	18-20				
SUS329J3L	0.03	1	2	0.04	0.03	4.5-6.5	21-24	2.5-3.5		0.08-0.5	
SUS821L1	0.03	0.75	2-4	0.04	0.02	1.5-2.5	20.5-21.5	0.6	0.5-1.5	0.15-0.2	
SUS821L1※	0.021	0.31	3.2	0.026	0	2.3	20.95	0.49	1.04	0.16	0.07

Table 2 Mechanical properties

Steel materials (JIS standard)	Yield strength (N/mm^2)	Tensile strength (N/mm^2)
SUS304	205	520
SUS329J3L	450	620
SUS821L1	400	600
SUS821L1※	517	689

Note: 0.2% offset strength was used for yield strength.
※ indicates the values from mill certificate.

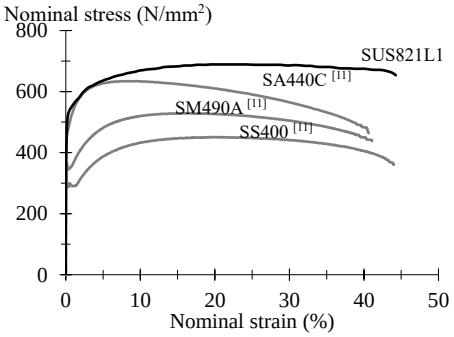

Fig. 1 Tensile test results

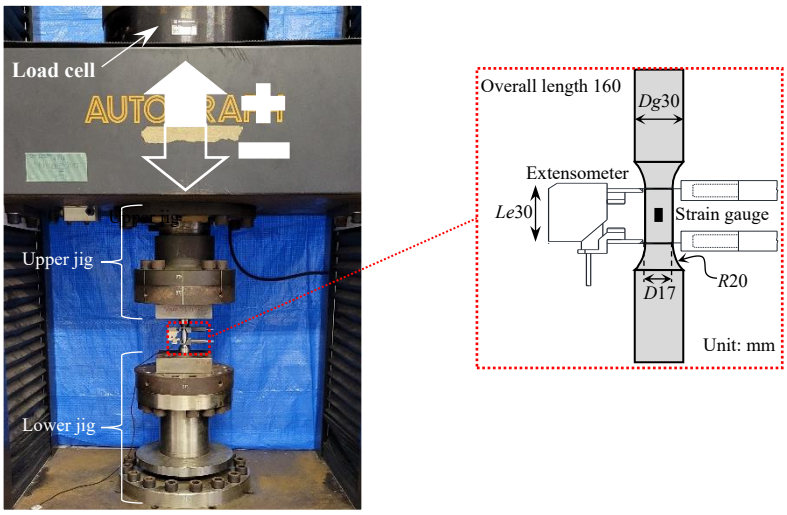

Fig. 2 Test setup

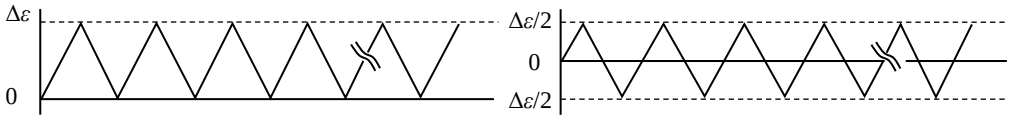

(a) Offset amplitude (SUS821L1 offset) (b) Fully reversed amplitude

Fig. 3 Loading history of constant stain amplitude

3 Low-cycle fatigue performances

3.1 Low-cycle fatigue performances of duplex stainless steel

Fig. 4 shows the relationship between the strain amplitude $\Delta\varepsilon/2$ and the number of cycles up to fracture N_f. The marks (■, □) in the figure represent the results obtained from constant amplitude cyclic loadings with offset and fully reversed amplitude, respectively. Fig. 4 shows that the LCF performance of SUS821L1 is independent of strain ratio for the range of strain amplitude and strain ratio considered in this study. The LCF performance evaluation equation for SUS821L1 lean duplex stainless steel is shown in Eq. (1).

$$\frac{\Delta\varepsilon}{2} = 0.0955(N_f)^{-0.409} \qquad (1)$$

To confirm the correspondence with the experimental results of the previous study [12], the test data obtained with a specimen of rectangular cross section made of S2205 duplex stainless steel are also shown in the figure with the mark (□). The S2205 steel corresponds to SUS329J3L of the JIS standard and S32205 of the U.S. UNS standard. The gray dotted line in the figure is extended using Equation (1). Fig. 4 indicates the LCF performance of the SUS821L1 and S2205 show a good linear relationship over a wide range of strain amplitudes, despite the difference in specimen geometries.

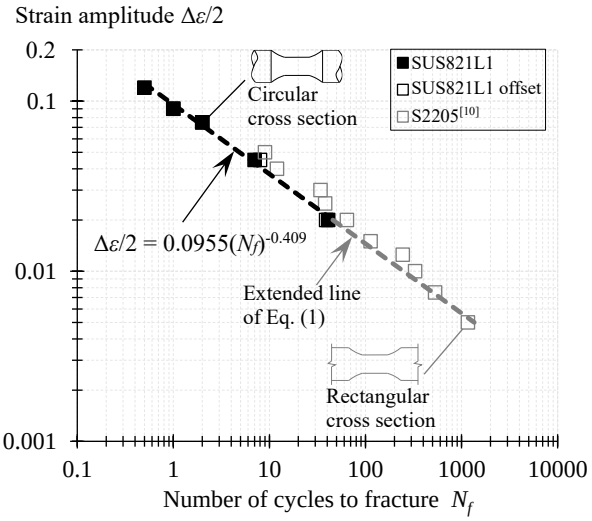

Fig. 4 LCF performances of SUS821L1 lean duplex and S2205 duplex stainless steels

3.2 Low-cycle fatigue performances of various steel materials

Fig. 5 shows the LCF performance of SUS821L1 comparing with that of other steels, which were used in previous studies [10,11]. S304 steel corresponds to SUS304 in the JIS standard and S30400 in the U.S. UNS standard.

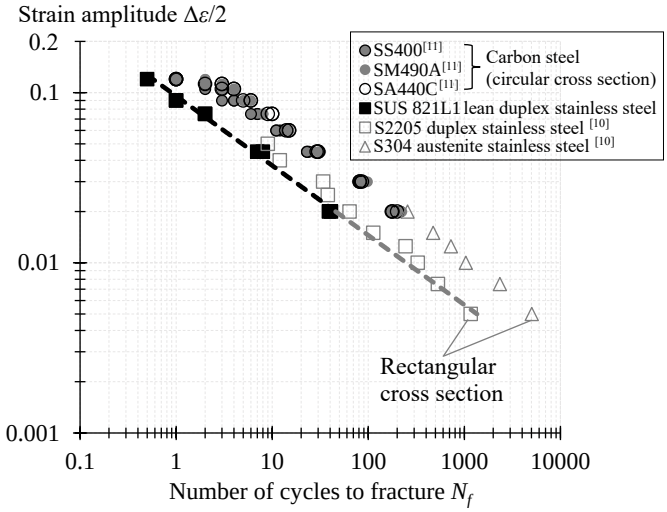

Fig. 5 LCF performances of various steel materials

The experimental results for carbon steel and austenitic stainless steel show good linear relationship and showing almost the same slope as the LCF performance curve for S2205 duplex stainless steel.

It is also noted that the duplex stainless steels have higher monotonic tensile strength than carbon and austenitic stainless steels (as shown in Fig. 1 and Table 1), but it has lower low-cycle fatigue performance as can be observed from Fig. 5. This trend was also reported in the previous study on the LCF performances of austenitic and duplex stainless steels [10].

On the other hand, the previous study [13] stated that in European standards, the evaluation formula of carbon steel may be used to evaluate the fatigue strength of stainless steels, although there are some limitations. However, Fig. 5 confirms that it is not appropriate to use the same evaluation formula as carbon steel to evaluate LCF performance of duplex stainless steel in the LCF region including large strain.

4 Differences in LCF performance from the perspective of skeleton curve and Bauschinger part decomposed from hysteretic curve

In this section, the differences in low-cycle fatigue (LCF) performance between SUS821L1 lean duplex stainless steel and (SS400, SM490A, SA440C) carbon steel [11] are discussed in terms of skeleton curves and Bauschinger parts decomposed from the hysteretic curve. It has been shown by bending and axial cyclic loading experiments that the plastic deformation performance of steel up to ductile fracture is strongly related to the proportion of skeleton curve and Bauschinger part in the hysteretic curve [14, 15]. To examine the difference in LCF performance in terms of hysteretic curve decomposition, the true stress ${}_t\sigma$ - true strain ${}_t\varepsilon$ relationship is first obtained.

4.1 True stress-true strain relationship

True stress and true strain are calculated using Eqs. (3) and (4) under the assumption of constant volume. The nominal stress σ_n in these equations is obtained by dividing the axial force acting on the specimen by the original cross-sectional area of the effective length section. While the nominal strain ε_n in the equations is obtained by dividing the length change occurring in the effective length section *Le* by the original length.

$$ {}_t\varepsilon = \ln(1 + {}_n\varepsilon) \qquad (3) $$

$$ {}_t\sigma = (1 + {}_n\varepsilon) \cdot {}_n\sigma \qquad (4) $$

Fig. 6 shows the true stress-true strain relationship at ±2%, ±9%, and ±12% constant amplitude cyclic loading tests for the lean duplex stainless steels and carbon steel. This figure shows that true stresses in tension and compression are almost symmetrical, and the stable true stress-strain relationship can be observed from small to large amplitude for the steel materials considered in this paper.

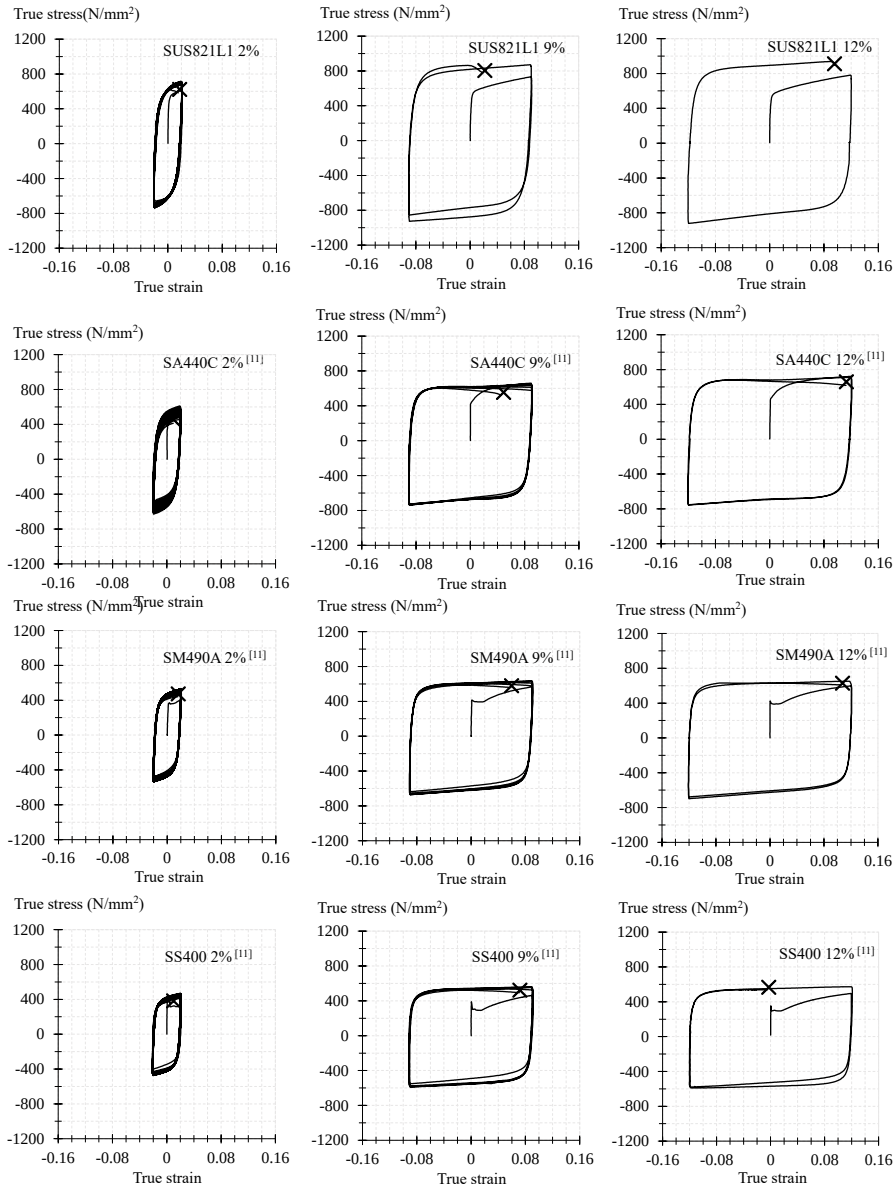

Fig. 6 True stress- true strain hysteretic curve

4.2 Decomposition of hysteretic curve

The true stress-true strain relationship is decomposed into the skeleton curve (hereinafter referred to as the skeleton part), the Bauschinger part, and the elastic unloading part [16], as shown in Fig. 7. Where E is the elastic stiffness of the steel, $\Delta_t\varepsilon_S^+$ and $\Delta_t\varepsilon_S^-$ are the increments of plastic strain in the skeleton part at each cycle on the tensile and

compressive side, respectively. $\Delta_t\varepsilon_B^+$ and $\Delta_t\varepsilon_B^-$ are the increments of plastic strain in the Bauschinger part. $\Sigma_t\varepsilon_S$ and $\Sigma_t\varepsilon_B$ are the cumulative plastic strains of the skeleton and Bauschinger parts. ${}_tW_S$ and ${}_tW_B$ are the plastic strain energies of skeleton and Bauschinger parts. W_t is the sum of ${}_tW_S$ and ${}_tW_B$. The skeleton curves are the sum of the increments of the true stress - true strain hysteretic curve at the first stress level reached in the compressive and tensile regions, respectively.

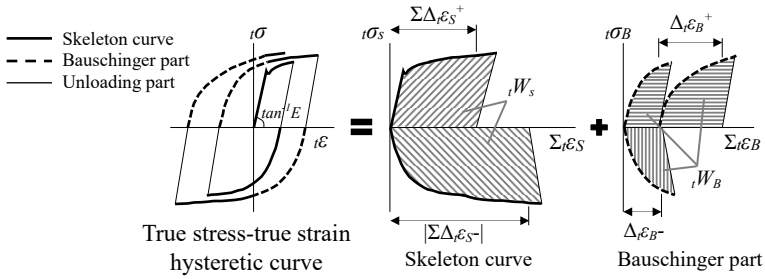

Fig. 7 Decomposition of hysteretic curve [16]

4.3 Effect of skeleton part on LCF performance

For all steels, as the strain amplitude increases, the plastic strain energy in the skeleton increases (Fig. 8), while the overall plastic strain energy tends to decrease (Fig. 9). In particular, the skeleton part of SUS821L1 shows the most significant plastic strain energy compared to those of carbon steels (Figs. 8 and 10). Since the skeleton part greatly affects the damage of the steel material, this could be one of the reasons why SUS821L1 has a low number of cycles to fracture, as seen in Fig. 5.

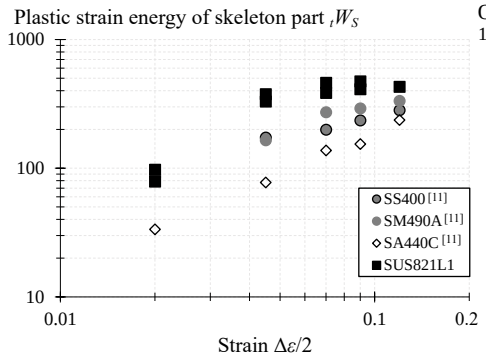

Fig. 8 Plastic strain energy of skeleton part at each strain amplitude

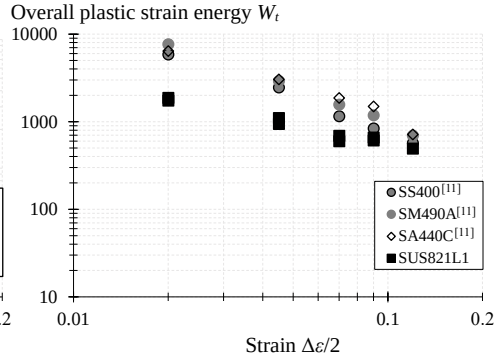

Fig. 9 Overall plastic strain energy at each strain amplitude

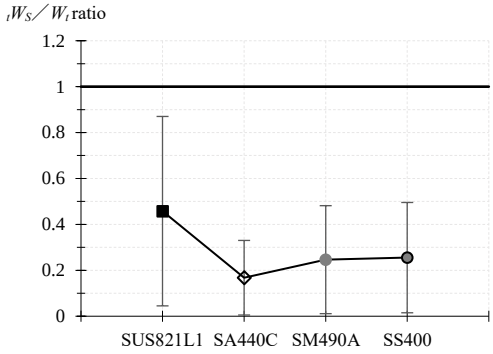

Fig. 10 Skeleton to overall plastic strain energy at each strain amplitude

4.4 Effect of Bauschinger part on LCF performance

For SS400 and SM490A steel materials in Fig. 11, the plastic strain at the Bauschinger part in each cycle is about the same. In contrast, for SA440C, the Bauschinger part appears the largest in each cycle due to its early stage of cyclic softening behavior [11], which is closely associated with the effect of heat treatment to achieve high strength.

Besides, it is observed from Fig. 8 that the plastic strain energy of the skeleton part for SA440C is small, while the overall plastic strain energy is comparable to that of SS400 and SM490A in Fig. 9. This implies that ignoring the Bauschinger part of the SA440C results in a significant underestimation of the energy absorption capacity of the steel material. Whereas considering the Bauschinger effect results in an evaluation of the energy absorption capacity comparable to that of SS400 and SM490A steels.

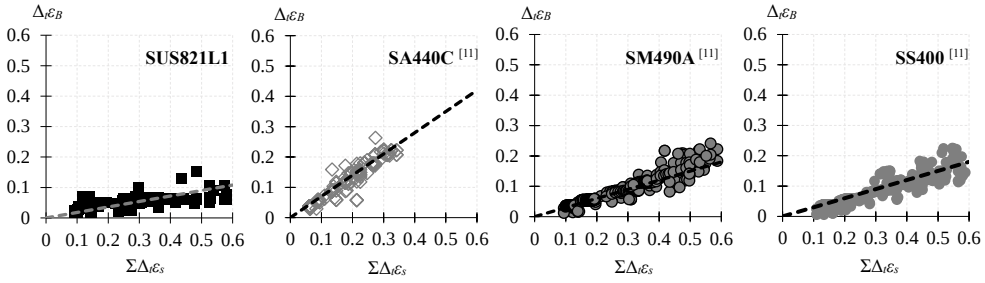

Fig. 11 Relationship between accumulated strain $\Delta_t\varepsilon_B$ and Bauschinger part in each cycle $\Sigma\Delta_t\varepsilon_S$

Conclusions

In this study, the low-cycle fatigue (LCF) performance including large strain of SUS821L1 lean duplex stainless steel was investigated. The results obtained in this study were compared with previous data of (S2205) duplex stainless steel, (S304) austenitic stainless steel and (SS400, SM490A, SA440C) carbon steels. It was confirmed the LCF performance of the lean duplex stainless steels of this study and the duplex stainless steels of previous studies showed good correspondence in a wide range of

strain amplitudes from small (±2%) to large (±12%). Although having higher yield points and tensile strengths than austenitic stainless steels and carbon steels, lean duplex and duplex stainless steels have lower LCF performance. Also, it was confirmed the effects of different steel materials on LCF can be explained in terms of skeleton curves and Bauschinger parts decomposed from the hysteretic curves.

Acknowledgements

The SUS821L1 lean duplex stainless steel used in this study was provided by the Japanese Society of Steel Construction.

References

1. Okada N, Tadokoro Y, Tsuge S, Gonome F, Kizaki M (2017) Lean Duplex Stainless Steel for Resources Saving Society, Zairyou-to-kankyo, Vol.66, No.8, pp.263－267.
2. JIS (Japanese Industrial Standards) G 4304. 2015. Hot-rolled stainless steel plate, sheet and strip.
3. Tateishi K, Hanji T (2004) Low cycle fatigue strength of butt-welded steel joint by means of new testing system with image technique, International journal of fatigue, Vol.26, pp.1349–1356, 2004.
4. He Q, Chen Y, Ke K, Yam MCH, Wang W (2019) Experiment and constitutive modeling on cyclic plasticity behavior of LYP100 under large strain range, Construction and building materials, Vol. 202, pp.507–521.
5. Udo R, Nishikawa H A, Haro H, Miyazaki K, Masaki K, Numakura H (2017)Effect of Loading Method and Mean Stress on Fatigue Strength of Super Duplex Stainless Steel, Tetsu-to-Hagane, Vol.103, No.4, pp.201-207.
6. Horisawa E, Sugiura K, Kitane Y (2021) Study on Fatigue Strength of Lean Duplex Stainless Steel Base Metal, Steel construction engineering, Vol.28, No.111, pp.107-117.
7. Alvarez-Armas I (2010) Low cycle fatigue behavior on duplex stainless steels, Transactions of the Indian institute of metals, Vol.63, Issue 2, pp.159–165.
8. Zhang M, Zheng B, Wang J, Wu B, Shu G (2022) Study on fracture properties of duplex stainless steel and its weld based on micromechanical models, Journal of constructional steel research, Vol.190, Article107115.
9. Chang X, Yang L, Zong L, Zhao M H, Yin F (2019) Study on cyclic constitutive model and ultra low cycle fracture prediction model of duplex stainless steel, Journal of constructional steel research, Vol.152, pp.105-116.
10. Chen L, Yao X, Sun Z, Wang D (2022) Study seismic performance of duplex stainless steel under large strain amplitude by cyclic loading test, Journal of constructional steel research, Vol.194, Article107332.
11. Yamada S, Touch T, Jiao Y, Kishiki S (2023) Cyclic deformation capacity of structural steels for earthquake-resistant steel buildings, Journal of earthquake engineering, pp.1-20.
12. Yamada S, Touch T, Jiao Y, Ishida T, Kishiki S: Deformation capacity of 400 N/mm^2 class structural steel under extremely large strains, Journal of constructional steel research, Vol.182, Article106678, 2021.

13. Gardner L (2005) The use of stainless steel in structures, Progress in Structural Engineering and Materials, Vol.7, Issue 2, pp.45-55.
14. Yamada S, Jiao Y, Kishiki S, Shibata A (2010) Plastic deformation capacity of structural steel under various axial strain histories, Journal of structural and construction engineering (Transactions of AIJ), Vol.75, No.656, pp.1909-1916.
15. Akiyama H, Takahashi M, Shi Z (1995) Ultimate energy absorption capacity of round-shape steel rods subjected to bending, Journal of structural and construction engineering (Transactions of AIJ), Vol.60, No.475, pp.145-154.
16. Kato B, Akiyama H, Yamanouchi Y (1973) Predictable properties of material under incremental cyclic loading. In Proceedings of LABSE symposium on resistance and ultimate deformability of structures acted on by well defined repeated loads, pp. 119–124.